Eur. Phys. J. B **45**, 203–206 (2005)
DOI: 10.1140/epjb/e2005-00055-1

THE EUROPEAN PHYSICAL JOURNAL B

Exchange bias studies of NiFe/FeMn/NiFe trilayer by ion beam etching

V.K. Sankaranarayanan[1,2], D.Y. Kim[1], S.M. Yoon[1], C.O. Kim[1], and C.G. Kim[1,a]

[1] Department of Materials Engineering & ReCAMM, Chungnam National University, 305-764 Daejeon, South Korea
[2] Microstructure Devices Group, Electronic Materials Division, National Physical Laboratory, Dr. K.S. Krishnan Marg, New Delhi-110012, India

Received 12 September 2004 / Received in final form 15 December 2004
Published online 8 March 2005 –

Abstract. Effect of low energy ion beam etching on exchange bias in NiFe/FeMn/NiFe trilayer is investigated in multilayers prepared by rf magnetron sputtering. Stepwise etching and magnetization measurement of FeMn layer in an NiFe/FeMn bilayer show increase of bias as etching proceeds and FeMn thickness decreases. The bias show a maximum around 7 nm FeMn thickness and then fall sharply below 5 nm, broadly in line with the exchange bias variation at increasing FeMn thickness but in reverse order, particularly at low FeMn thickness. Progressive etching of top NiFe layer in the NiFe/FeMn/NiFe trilayer shows an initial gradual increase in bias followed by a sharp increase below 7 nm thickness of top NiFe layer, with a maximum at 2 nm thickness for both NiFe layers and greater bias for seed NiFe layer.

PACS. 75.70.Cn Magnetic properties of interfaces (multilayers, superlattices, heterostructures) – 75.60.Ej Magnetization curves, hysteresis, Barkhausen and related effects – 75.30.Et Exchange and superexchange interactions

1 Introduction

Exchange bias phenomenon has continued to fascinate magnetism researchers ever since its discovery four decades ago but its microscopic origin remains a mystery despite intense research efforts in the past decade [1,2]. Exchange bias is often attributed to the presence of interfacial uncompensated spins, which are believed to have a structural origin in surface and interface roughness [3]. Ion beams could be utilized to get useful insight into the surface and interface properties in nanostructured multilayers wherein layers are of nano or sub-nanometer thickness. Recent studies show that He ion beams in the few keV range have a remarkable effect on the exchange bias in a variety of multilayer systems [4]. Ar ion beam etching is a low energy process in the sub keV range often employed for dry etching of surfaces in multilayers. It is inevitable to introduce etching induced microstructural changes in materials due to the physical nature of the etching process, i.e., ion bombardment, but it is not known whether the magnetic properties are affected by such low energy ion bombardment.

FeMn is widely used AFM (antiferromagnet) layer for exchange bias in spin valve structures in spite of its relatively low blocking temperature and corrosion resistance, in comparison to the more expensive IrMn, PtMn and other AFM materials with more desirable properties [1]. FeMn needs to be deposited onto an fcc seed layer such as NiFe, or Cu in order to crystallize the antiferromagnetic γ-fcc phase [5,6]. In the absence of seed layers low exchange bias around 50 Oe is reported even after field annealing [7]. When NiFe is used as the seed layer, many of the spin valve structures with FeMn as AFM layer consist of a NiFe/FeMn/NiFe trilayer structure where the bottom NiFe is the seed layer and the top NiFe layer forms the pinned layer. This trilayer shows two biased hysteresis loops with different bias owing to the presence of two AFM/FM interfaces and is a unique system to study exchange bias. Exchange bias being an interfacial property many of the conventional measurement techniques are ineffective in its study. In this study we have investigated the effect of Ar ion beam etching of FeMn layer in an NiFe/FeMn bilayer and the top NiFe layer in a NiFe/FeMn/NiFe trilayer on exchange bias.

2 Experimental procedure

The multilayer thin films of the following compositions I: $Si/SiO_2/Ta(5)/NiFe(10)/FeMn(20)$, II: $Si/SiO_2/Ta(5)/NiFe(5)/FeMn(10)/NiFe(t)/Ta(5)$ (nm), where t is in the range of 2 to 20 nm, were prepared by rf magnetron sputtering at a base vacuum around 3×10^{-7} torr. Argon gas pressure was 1×10^{-3} torr.

[a] e-mail: cgkim@cnu.ac.kr

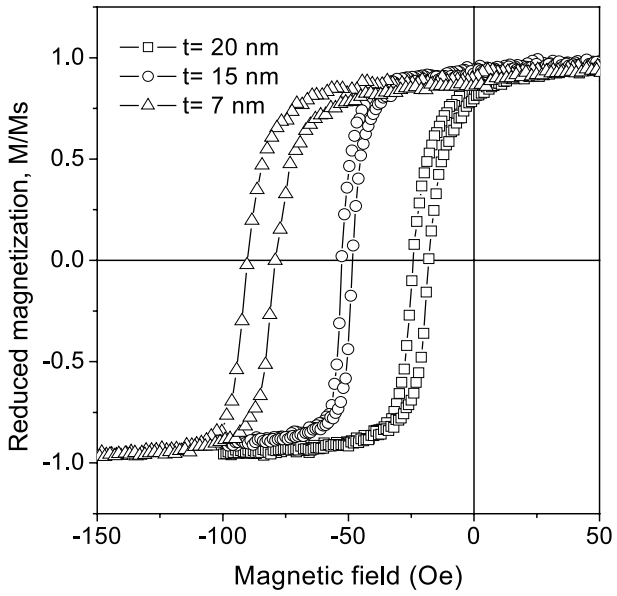

Fig. 1. Magnetic hysteresis loops of etched Ta/NiFe(10)/FeMn(t) (nm) films at IBE voltage of 500 V.

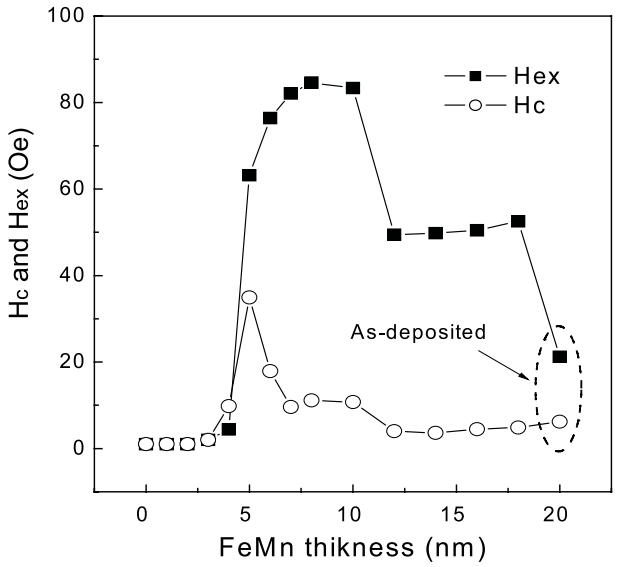

Fig. 2. The variation of exchange bias and coercivity in NiFe/FeMn bilayer as a function of decreasing FeMn thickness during etching.

There was no magnetic field applied during etching. The deposition rates of all the layers were around 0.1 nm/s. A constant magnetic field of 60 Oe was applied at the time of film deposition to develop the necessary exchange bias. No additional field annealing and cooling was carried out.

VSM measurements were carried out on a LDJ 9600 magnetometer. A Kaufman type ion source was used to generate Ar ion beam and a beam tilt angle of 20 and a beam acceleration voltage of 500 V were employed during etching. The ion source-substrate distance was 20 cm. Top NiFe or FeMn layer was etched followed by exchange bias measurements at every etching step. The main factors affecting the etching rate and magnetic

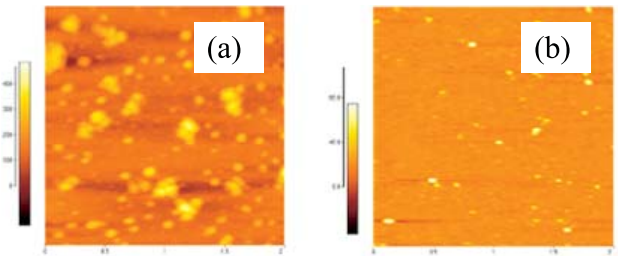

Fig. 3. AFM micrographs of FeMn layer, (a) as-deposited (RMS roughness: 3.15 A), (b) after etching (RMS roughness: 1.95 A).

properties of the films are considered to be the amount of accelerated ion flux and the kinetic energy of the ion, which are dominated by beam voltage and beam current.

3 Results and discussion

The XRD patterns of the multilayered samples showed (111) texture for both FeMn and NiFe layers necessary for the development of γ-FeMn antiferromagnetic phase and exchange bias [8].

We first did ion beam etching of the FeMn layer in a NiFe(10 nm)/FeMn(20 nm) bilayer system with the multilayer of composition I. Figure 1 shows the magnetic hysteresis loops at different FeMn thickness; t = 20 nm (as-deposited) and reduced thickness t = 7 and 15 nm after etching. We can see the shift of loop as etching proceeds, reducing the FeMn thickness. The exchange bias field in Figure 2, after an initial rapid increase at the initiation of etching remains nearly constant down to a thickness of 12 nm, increases again to reach its maximum value around 7 nm and falls finally below 5 nm thicknesses. The coercivity also follows a similar increase with decreasing FeMn thickness as etching proceeds and shows a sharp maximum at low FeMn thickness near the critical thickness for the onset of exchange bias.

The behavior of both exchange bias and coercivity are broadly similar to the thickness dependence of exchange bias observed in the studies where deposited FeMn thickness is gradually increased [9]. Exchange bias is an interface phenomenon and is often considered to depend on roughness at interfaces [3] as well as grain size dominating domain size [10,11]. Figure 3 shows the comparison of surface roughness measured by AFM between as-deposited and FeMn surface etched 5 nm. The RMS roughness of 3.15 A for as-deposited sample is reduced to 1.95 A for 5 nm etched one. Figure 4 shows the XRD patterns for as-deposited and 5 nm etched samples. Using Scherrer equation [12], the grain size from these patterns is evaluated to be 9.5 nm for as-deposited, and 8.2 nm for etched samples.

It is hard to know the surface roughness effect on exchange bias because it is not easy to coorelate the interfacial roughness with surface roughness. However, the increase of exchange bias with etching can be understood by the decrease of grain size. The sharp drop in exchange bias at 5 nm of FeMn thickness could be due to the

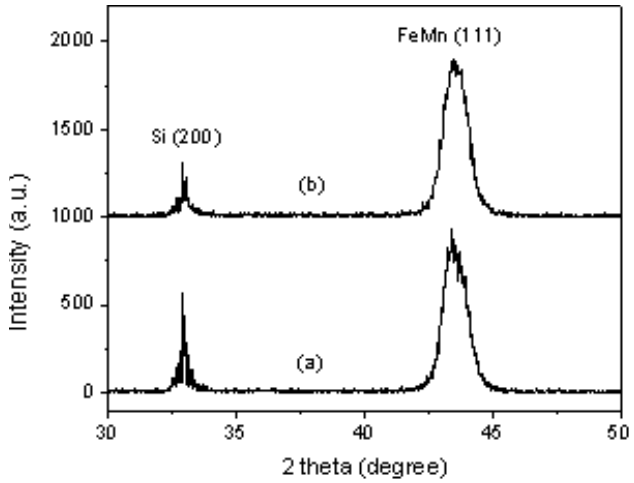

Fig. 4. XRD patterns of FeMn layer, (a) as-deposited (grain size: 9.5 nm), (b) after etching (grain size: 8.2 nm).

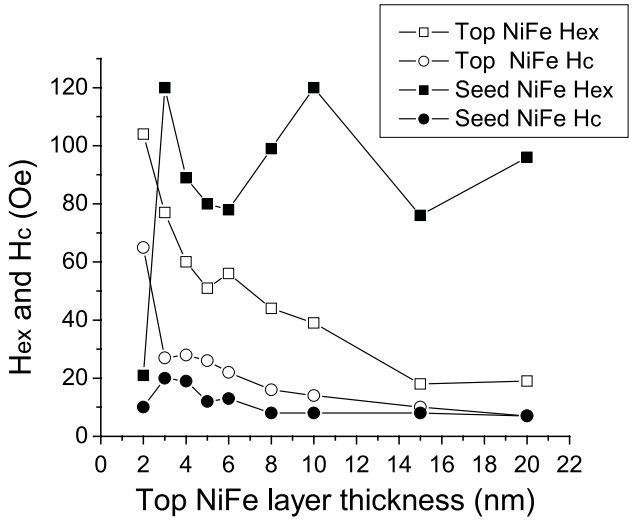

Fig. 5. Exchange bias and coercivity of the trilayer as a function of as-deposited top NiFe layer thickness.

rotatable magnetic anisotropy of FeMn materials, which is revealed for thinner AFM layer thickness than critical value of ∼6 nm [9,13].

Increasing thickness of the top NiFe layer in a NiFe/FeMn/NiFe trilayer, for constant seed NiFe layer and FeMn thickness of 5 nm and 10 nm respectively, shows variation of exchange bias for the two NiFe layers as shown in Figure 5. The seed NiFe layer shows greater bias than the top NiFe layer with an oscillatory type variation, in the whole thickness range, as seen. The bias for the top NiFe layer shows a steady $1/t$ fall with increasing thickness t. The coercivity for both NiFe layers show maxima in the low thickness range of 2−4 nm and then fall steadily with increasing thickness.

In order to investigate the effect of ion beam etching on exchange bias of the two NiFe layers of the trilayer, we took a trilayer sample with a top NiFe layer thickness of 20 nm (i.e., (Ta(5)/NiFe(5)/FeMn(10)/NiFe20), etched it in steps of 2 nm and recorded the magnetization curves

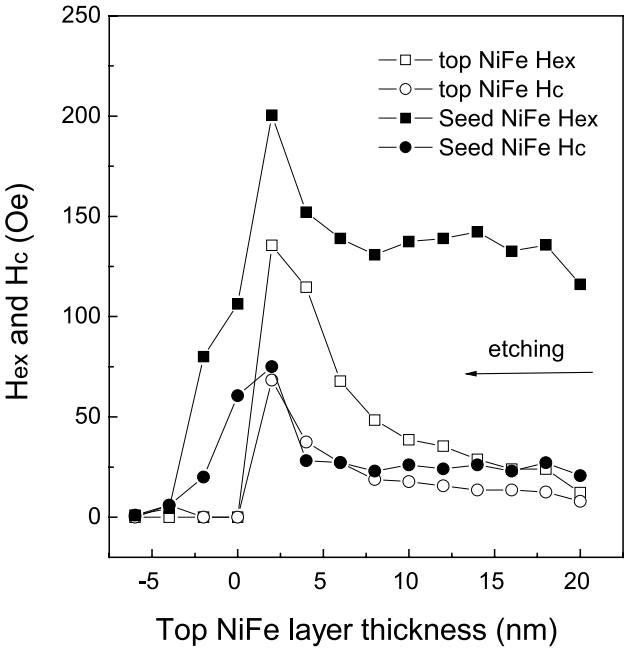

Fig. 6. Exchange bias and coercivity variations as a function of top NiFe layer thickness after etching.

at every step and plotted the exchange bias and coercivity of the two hysteresis loops corresponding to the seed and top NiFe layers in Figure 6. Before etching, the bottom NiFe layer shows an exchange bias of 120 Oe and the top NiFe layer about 20 Oe, as seen in figure. When compared to the respective bias curves for the seed and top NiFe layers for increasing thickness of top NiFe layer in Figure 5, it is evident that the decreasing thickness by etching of top NiFe layer from 20 nm does not follow similar path. The oscillatory type behaviour of bias observed for seed NiFe layer in Figure 5 is not evident, which is presumably due to the fluctuations in the texture and grain size. The bias in fact has a nearly constant value around 140 Oe in the 18 to 12 nm thickness and thereafter increases sharply to reach 200 Oe around 2 nm thickness. Though the maximum bias for seed layer is observed around the same thickness of 2−3 nm, the bias value observed is much larger after etching, for both seed and top NiFe layers in comparison with that in Figure 5.

The bias for the top NiFe layer shows a steady increase from its minimum value at 20 nm thickness to reach its maximum around 2 nm thickness, which again is greater than the corresponding maximum in Figure 1. The increase of exchange bias of the top NiFe layer with etching could be related with $1/t$-dependence with decreasing thickness t.

The increase in bias of the order of 80 Oe observed for both the seed and top NiFe layers after ion beam etching shows that the low energy ion beam etching is also capable of enhancing the bias as observed in the case of He ion irradiations [4], while retaining the multilayer characteristics and magnetic properties. The enhancement may be the result of the defects induced in the antiferromagnet as result of bombardment with Ar ions, which are heavier

than He ions, though lower in energy. These defects may serve as energetically favourable pinning sites for magnetic domain formation and increase in the number of domains and bias as described in the case of dilution of antiferromagnet which leads to a substantial enhancement in bias [9].

Conclusions

Ion beam Etching of the FeMn layer of a NiFe/FeMn bilayer with an FeMn thickness of 20 nm shows a maximum in exchange bias around 7 to 10 nm thickness followed by a sharp fall at low FeMn thickness. The RMS roughness of 3.15 A for as-deposited sample is reduced to 1.95 A for 5 nm etched one, and the grain size is reduced to 8.2 nm from 9.5 nm after etching. The etching of the top NiFe layer in the NiFe/FeMn/NiFe trilayer shows an initial gradual increase in bias of seed NiFe layer with decreasing top NiFe, followed by a sharp increase at top NiFe thickness of 2−3 nm. The bias field of top NiFe has similar variation tendency with smaller bias than that of seed NiFe layer.

This work was supported by the KOSEF through ReCAMM and R01-2003-000-10644-0, and by the KRF through the BK21 program.

References

1. J. Nogues, I.K. Schuller, J. Magn. Magn. Mater. **192**, 203 (1999)
2. A.E. Berkowitz, K. Takano, J. Magn. Magn. Mater. **200**, 552 (1999)
3. K. Takano, R.H. Kodama, A.E. Berkowitz, W. Cao, G. Thomas, J. Appl. Phys. **83**, 6888 (1998)
4. D. Engel, A. Kronenberger, M. Jung, H. Schmoranzer, A. Ehresmann, A. Paetzold, K. Roll, J. Magn. Magn. Mater. **263**, 275 (2003)
5. G. Choe, S. Gupta, Appl. Phys. Lett. **70**, 1766 (1997)
6. H. Sang, Y.W. Du, C.L. Chien, J. Appl. Phys. **85**, 4931 (1999)
7. M. Xu, Z. Lu, T. Yang, C. Liu, Z. Mai, W. Lai, Q. Jia, W. Zheng, J. Appl. Phys. **92**, 2052 (2002)
8. V.K. Sankaranarayanan, S.M. Yoon, D.Y. Kim, C.O. Kim, C.G. Kim, J. Appl. Phys. **96**, 7428 (2004)
9. R. Jungblut, R. Coehoorn, M.T. Johnson, J.A. de Stegge, A. Reinders, J. Appl. Phys. **75**, 6659 (1994)
10. Z. Lu, W. Lai, C. Chai, Thin Solid films **375**, 224 (2000)
11. A.P. Malozemoff, J. Appl. Phys. **63**, 3874 (1988)
12. L.S. Birks, H. Friedman. J. Appl. Phys. **17**, 687 (1946)
13. J. Nogues, I.K. Schuller, J. Magn. Magn. Mater. **17**, 203 (1999)
14. P. Miltenyi, M. Gierlings, J. Kellr, B. Beschotten, G. Guntherodt, U. Nowak, K.D. Usadel, Phys. Rev. Lett. **84**, 4224 (2000)